Effective glucose metabolism maintains low intracellular glucose in airway epithelial cells after exposure to hyperglycaemia.

Jade Bearham[1], James P. Garnett[2,3], Victoria Schroeder[3], Matthew GS Biggart[1], Deborah L. Baines[1]

[1] Institute for Infection and Immunity, St George's University of London, London SW17 0RE, UK, [2] Institute of Cellular Medicine, Newcastle University, Newcastle upon Tyne, NE1 7RU UK, [3] Immunology & Respiratory Diseases Research, Boehringer Ingelheim Pharma GmbH & Co. KG, Birkendorfer Str. 65, 88397 Biberach an der Riß, Germany. .

Running Title: Glucose metabolism in airway epithelial cells

Abstract

The airway epithelium maintains differential glucose concentrations between the airway surface liquid (ASL, ~0.4mM) and the blood/interstitium (5-6mM) which is important for defence against infection. Glucose primarily moves from the blood to the ASL via paracellular movement, down its concentration gradient, across the tight junctions. However, there is evidence that glucose can move transcellularly across epithelial cells. Using a Förster Resonance Energy Transfer (FRET) sensor for glucose, we investigated intracellular glucose concentrations in airway epithelial cells and the role of hexokinases in regulating intracellular glucose concentrations in normo- and hyperglycaemic conditions. Our findings indicated that in airway epithelial cells (H441 or primary human epithelial cells HBEC) exposed to 5mM glucose (normoglycaemia), intracellular glucose concentration is in the μM range. Inhibition of facilitative glucose transport (GLUT) with Cytochalasin B reduced intracellular glucose concentration. When cells were exposed to 15mM glucose (hyperglycaemia), intracellular glucose concentration reduced. Airway cells expressed hexokinases I, II and III. Inhibition with 3-bromopyruvate decreased hexokinase activity by 25% and elevated intracellular glucose concentration but levels remained in the μM range. Exposure to hyperglycaemia increased glycolysis, glycogen and sorbitol. Thus, glucose enters the airway cell via GLUT transporters and is then rapidly processed by hexokinase-dependent and hexokinase independent metabolic pathways to maintain low intracellular glucose concentrations. We propose this prevents transcellular transport, aids the removal of glucose from the ASL and that the main route of entry for glucose into the ASL is via the paracellular pathway.

Introduction

Glucose concentrations in the airway surface liquid (ASL) of a healthy individual are typically 0.4mM; 12.5x lower than plasma glucose concentrations (5mM), but this has been shown to rise during periods of hyperglycaemia and inflammation (1, 31). Previous studies have shown that the appearance of glucose in the ASL is largely reliant on paracellular movement of glucose via tight junctions, down its concentration gradient (19, 30). However, there is some evidence that glucose can also move transcellularly across the airway epithelium from the blood to the ASL via glucose transporters in the cellular membrane (19, 22, 30). Such a process is found in other systems such as the intestine and the kidney (where glucose moves from the lumen to the blood) although the gradient driving transcellular movement of glucose in these tissues is in the opposing direction to that of the lung (16, 27). We hypothesised that transcellular movement of glucose in the airway is largely dependent on the intracellular concentration of glucose which is regulated by hexokinase activity. Low intracellular glucose maintains a driving force for glucose to enter the cell. However, if intracellular glucose concentrations rise to that of ASL or higher, for example during exposure to hyperglycaemia, this would promote luminal efflux of glucose. Understanding the routes for glucose movement across the airway epithelium is vital because an increase of glucose in the ASL has been associated with increased airway infections in respiratory disease (3, 5).

Glucose Förster Resonance Energy Transfer (FRET) sensors have been developed to exhibit a change in fluorescence output upon glucose binding, indicating a change in local glucose concentrations. These sensors have been used to measure intracellular glucose concentrations in systems such as ovarian epithelial cells (4) and glucose fluxes in pancreatic β cells (21). To

our knowledge, intracellular glucose concentrations in airway epithelial cells and the metabolic processes regulating intracellular glucose concentrations have not yet been investigated.

In this study, we used a FRET sensor to measure intracellular glucose concentrations in airway epithelial cells in normo- and hyper-glycaemic conditions. We also investigated the involvement of hexokinases in regulating intracellular glucose concentration, airway cell glucose metabolism and the effect on ASL glucose concentrations.

Materials and methods

Cell culture

H441 airway epithelial cells were cultured at 37^0C, 5% CO_2 in RPMI 1640 media containing 10mM glucose and supplemented with 10% Foetal calf serum (Sigma Aldrich, USA), 2mM L-glutamine, 1mM Sodium pyruvate, 5µg/ml insulin, 2.75µg/ml penicillin and 100mg/ml streptomycin (Life Technologies, USA). Human bronchial epithelial cells HBEC cells were originally purchased from Lonza and Epithelix SàRL prior to semi-immortalization with BMI-1 transduction and were cultured in collagen coated flasks (Corning) in bronchial epithelial growth media (BEGM; Lonza) in a humidified environment at 37^0C, 5% CO_2. Growth media was replaced every second day, and cells were passaged once 80% confluent.

Polarised monolayers were cultured on Transwells (Corning, USA). H441 cells were plated onto the Transwell using the medium described above until confluent. The apical medium was then removed and the basolateral medium was changed to RPMI 1640 media containing 10mM glucose and supplemented with 4% charcoal stripped serum, 200µM dexamethasone,

10nM 3,3'-5-triiodothyronine, 2mM L-glutamine, 1mM sodium pyruvate, 5µg/ml insulin, 2.75µg/ml penicillin and 100mg/ml streptomycin. Cells were then cultured at air-liquid interface (ALI) for 10 days, changing the medium every other day until they formed a resistive monolayer. HBEC were seeded at a density of 200,000 cells cm^{-2} on Transwells. After confluence was achieved, media was removed from the apical surface and the cells were fed on the basolateral side only with 50% BEGM and 50% Hi-glucose minimal essential medium containing 100 nM retinoic acid. The media was exchanged every 2 to 3 days and the apical surface mucus was removed by gentle washing with phosphate-buffered saline once a week. Cultures were used for functional analysis 28-35 days after exposure to ALI. BMI-1 transduced cells exhibit normal cell morphology, karyotype, and doubling times despite extensive passaging. When cultured at ALI they show normal ciliation, production of MUC5AC, MUC5B and have electrophysiological properties similar to primary cells (26). Transepithelial resistance was measured before use with an epithelial volt/ohm meter EVOM (Word Precision Instruments) and at least 200 Ωcm^2 was required before use in experiments. 18 hours prior to experiments, cell media was exchanged with growth medium containing 5mM D-glucose (supplemented as listed above). To investigate the effect of hyperglycaemia, cells were either exposed to 5mM D-glucose + 10 mM L-glucose (an analogue not transported or metabolised to control for any osmotic effects of raising glucose), to mimic normoglycaemia (5mM glucose) or 15 mM D-glucose to mimic hyperglycaemia (15 mM glucose) -. The apical surface of cell cultures were gently washed with 100µl PBS to obtain airway surface liquid washes. Glucose in the washes was analysed using an amplex red glucose oxidase kit (ThermoFisher, UK).

Cell Transfection

Cells were seeded at a density of $2x10^5$ onto glass coverslips coated in poly-lysine and once at 50-65% confluency, were transiently transfected with 1µg of the glucose sensitive sensor FLII12Pglu-700µΔ6 (Addgene plasmid # 17866) or CFP-YFP FRET positive control plasmid (a kind gift from R. Tarran UNC, Chapel Hill[15]) using Lipofectamine 2000 (Thermo Fisher, UK). Polarised monolayers were apically transfected in a similar fashion, with 1µg of plasmid transfected using TransIT-X2 (Mirus, USA) applied to the apical surface of the cells.

FRET microscopy

Cells were imaged 48-72 hours post transfection in phosphate buffered saline at 37°C, 95% air/ 5% CO_2, supplemented with glucose and/or inhibitors using a Zeiss LSM 510 Meta confocal microscope with a 20x Pan-Neofluar lens, or a Leica SP8 with a 20x PL APO CS2 lens. FLII12Pglu-700µΔ6 contains the FRET paired fluorophores eCFP (donor) and citrine (acceptor) which reports a reduced eCFP/citrine FRET ratio with a binding of glucose. This was measured on the Zeiss LSM 510 by collecting emission data from eCFP (459-505nm) and citrine (525-600nm) every 4 seconds over an 8-minute time period whilst exciting eCFP at 458nm. Settings were optimised for the growth conditions of each cell type which took into account opacity of the substrate (ie glass coverslips, Transwells), cell height and density. Thus, the output measurement was different for the three conditions studied.

Generating dose response data for the sensor

Glucose dose response data was generated for each cell type and growth condition. Cells transfected with FLII12Pglu-700µΔ6 were treated with hexokinase inhibitor 3-Bromopyruvic acid (BrPy) (100µM) plus the respiratory chain complex I inhibitor, Rotenone (100nM) for

30 minutes to inhibit glucose metabolism. During this time cells were incubated with different glucose concentrations to equilibrate intracellular glucose with extracellular glucose prior to imaging as previously described to equilibrate intracellular and extracellular lactate for FRET measurement (33). FRET activity of FLII12Pglu-700μΔ6 was imaged as described above.

Hexokinase assay

Cells were untreated or pre-treated for 10 minutes with BrPy (0.1μM-1mM) at 37°C, 95% air/5% CO_2. Cell lysates were prepared and a colorimetric hexokinase assay (ab136957, Abcam, UK), which measures the conversion of glucose to glucose-6-phosphate by hexokinase, was performed as per the manufacturer's instructions.

Sorbitol assay

Proliferating H441 cells were exposed to 5mM D- + 10mM L- glucose or 15mM D-glucose in the presence or absence of BrPy (100μM) for 10 minutes prior to washing in ice-cold PBS. Cells were then lysed in 200μl of assay buffer and centrifuged for 5 minutes at 4°C at 12,000rpm. The lysate was decanted, and sorbitol concentrations were determined by sorbitol colourimetric assay (Abcam, ab118968) as per the manufacturer's protocol.

Seahorse Glycolysis Stress Assay

Human bronchiolar epithelial cells were seeded into a Seahorse XF96 plate and incubated at 37°C, 5% CO2 for 48 hours. The medium was changed 24 hours prior to Seahorse experiment and cells were exposed to 5 or 15 mM glucose with or without BrPy (100μM) or Epalrestat (1 or 10μM) for the last 30 minutes before the Seahorse Glycolysis Stress Assay was performed according to the manufacturer's instructions followed by the sequential injection of oligomycin to inhibit ATP-linked reparation and 2-Deoxy-D-Glucose (2-DG) to

inhibit glucose metabolism. The plate layout was separated into quadrants to reduce edge effects. Extracellular acidification rate (ECAR) and oxygen consumption rate (OCAR) were measured. Glycolysis rate was calculated by subtracting the normalized ECAR values after 2-DG injection from the ECAR values after glucose injection in order to exclude the non-glycolytic acidification from the calculation. Glycolytic capacity was calculated by subtracting the non-glycolytic acidification rate (ECAR after 2-DG injection) from the maximum ECAR after 1 μM oligomycin injection.

Western Blots

Cells were lysed in RIPA buffer (20 mM Tris-HCl (pH 7.5), 150 mM NaCl, 1 mM Na_2EDTA 1 mM EGTA, 1% NP-40, 1% sodium deoxycholate) plus protease inhibitor cocktail (Sigma, UK) with gentle agitation at 4°C, 30 minutes. Protein concentration was calculated from a BCA assay (Thermo Fisher, UK). 20μg of protein was electrophoresed through a 4-12% Bis-Tris gel. Gels were blotted onto a PVDF membrane and blocked with Odyssey blocking buffer (LiCor, USA). Membranes were incubated in primary antibodies (Hexokinase I: ab65069; 1:500, Hexokinase II: ab37593; 1:250, Hexokinase III: ab126217; 1:500, B-Actin: A5441, 1:10000) followed by secondary antibodies (goat-anti-rabbit 680RD: 925-68071, 1:15000 and donkey-anti-mouse 800CW, 925-32212, 1:15000). Blots were imaged using the LiCor Odyssey system.

Data analysis

FRET eCFP/citrine intensity and western blot band intensity data was measured using ImageJ software. Data are displayed as mean values ± standard deviation and analysed using GraphPad prism 7 using ANOVA followed by a post hoc Tukeys test unless otherwise stated.

Results

Hexokinase proteins I, II and III are present in airway epithelial cells

As glucose enters the cell it is phosphorylated by hexokinases to glucose-6-phosphate reducing the intracellular concentration of free glucose. Western blot of cell extracts from H441 cells grown on plastic (proliferating) or H441 and HBEC grown at air-liquid interface indicated the presence of hexokinases I, II and III in these cells. There was no observed difference in the total cellular abundance (hexokinase/actin) of these proteins in H441 cells after exposure to either 5mM or 15 mM glucose (Figure 1A&B).

Hexokinase activity in airway cells is reduced by BrPy

Addition of BrPy to H441 cells reduced total hexokinase activity in cell extracts in a dose dependant manner with an IC_{50} of 1.2±0.28 mM (Figure 2A). The data did not follow a classic sigmoid curve and there was an indication that the inhibition was biphasic. We were unable to unambiguously fit such a curve to the data. However, the IC_{50} obtained from the initial inhibition of hexokinase activity was lower at 0.04±0.01mM. As there was no statistical difference in hexokinase activity between pre-treatment with 100µM or 1mM, it was decided to use the lower concentration of BrPy. At this concentration total cellular hexokinase activity was reduced by 25.1 ± 11.6 % in H441 cells cultured at air-liquid interface (n=6) (Figure 2B).

Hexokinse activity drives glycolysis in airway cells

Using the seahorse assay, we previously showed that airway cells produce energy by mitochondrial respiration (OCR) and that elevation of extracellular glucose shifts metabolism to glycolysis (ECAR) which is associated with increased lactic acid secretion (12). We found that BrPy (100μM) was effective at inhibiting both mitochondrial respiration (Figure 3A) and glycolysis in these cells (Figure 3B&C). We calculated that BrPy inhibited glycolysis with an IC_{50} of 0.06 ± 0.02 mM (Figure 3D). Application of 2-DG, an inhibitor of all hexokinase activity was more effective at inhibiting respiration and glycolysis (Figures 3A,B,C) These data indicate that glycolysis is predominantly driven by hexokinase II activity in these cells.

Elevating extracellular glucose and inhibiting hexokinase activity changed FRET ratio in non-polarised, polarised H441 and HBEC.

Proliferating H441 cells transfected with FLII12Pglu-700μΔ6 and exposed to 5mM extracellular glucose, exhibited a cyclic fluctuation in FRET ratio of eCFP/citrine over time, with a full cycle taking 3.4 ± 0.2 minutes (n=16) (Figure 4A). This was not observed when the control FRET eCFP/citrine plasmid was transfected into cells (data not shown). Elevation of extracellular glucose to 15 mM resulted in an increase in FRET ratio from 1.54 ± 0.02 to 1.6 ± 0.02 ($p<0.0001$, n=117), indicating a decrease in intracellular glucose. In addition, the cyclic fluctuations slowed to 4.3 ± 0.3 minutes for a full cycle (n=16; $p<0.05$) Figure 4A. Pre-treatment with the hexokinase inhibitor BrPy decreased FRET from 1.54 ± 0.02 to 1.41 ± 0.01 ($p<0.0001$; n=117) indicating that intracellular glucose was increased (Figure 4A). Furthermore, BrPy prevented the large cyclic fluctuations in FRET indicating that hexokinase activity was associated with this phenomenon. As an alkylating agent, it is possible that BrPy could directly affect the sensor. However, this would likely reduce glucose binding or

stochiomic changes to the sensor, neither of which would explain these results. Thus, these data indicate that intracellular glucose concentration fluctuated with external glucose concentration and hexokinase activity.

H441 cells cultured at air-liquid interface on permeable supports required altered microscope conditions for FRET acquisition which meant that the measured FRET ratio of eCFP/citrine was decreased compared to that observed in proliferating cells. Nevertheless, in cells exposed to 5mM extracellular glucose the pattern of response was similar to that seen in proliferating cells. A cyclic fluctuation in FRET ratio was also observed in these cells with a full cycle taking 4.4 ± 0.6 minutes, in 5mM glucose. Elevation of extracellular glucose to 15mM resulted in an increased FRET ratio from 0.38 ± 0.007 to 0.41 ± 0.005 ($p<0.0001$, n=83) Addition of BrPy reduced FRET ratio to 0.34 ± 0.003 and the cycling frequency to 1.3 ± 0.23 minutes ($p\leq0.001$; n=16).

Optimisation of FRET acquisition in HBEC cultured at air-liquid interface also resulted in a change in FRET ratios obtained. However, similar to H441 cells, FRET ratio increased when extracellular glucose was increased from 5mM to 15mM ($p<0.0001$, n=149).

Inhibition of GLUT mediated glucose uptake increased FRET ratio in H441 cells grown at air-liquid interface.

Cytochalacin B is molecule larger than glucose, which binds to the pore of facilitative glucose transporters (GLUT) and blocks glucose uptake. Cytochalacin B treatment of H441 cells grown at air-liquid interface and exposed to 5mM or 15mM glucose significantly increased FRET ratio ($p<0.0001$, n=24 respectively). These data indicate that inhibition of glucose uptake into the cell reduced intracellular glucose (Figure 5).

Intracellular glucose concentration of H441 and HBEC.

A dose response curve for FRET ratio was generated for the three different cell/growth conditions using the individual imaging conditions used. An exemplar dose response curve for proliferating H441 cells is shown (Figure 4B). This was then used to interpolate the data points shown in Figure 4A to calculate the intracellular concentration of glucose. The mean intracellular glucose concentration for proliferating H441 cells in 5mM glucose was 0.23 ± 0.05mM. Raising the glucose concentration to 15mM glucose resulted in a decrease in intracellular glucose to 0.05 ± 0.04 mM. Pretreatment with BrPy increased intracellular glucose concentration to 0.49 ± 0.01 mM in 5mM and 0.46 ± 0.03 in 15 mM glucose ($p<0.0001$, n=117 compared to control respectively) (Figure 6A).

Interpolation of data from H441 cells cultured at air-liquid interface indicated that these cells has a mean intracellular glucose of 0.36 ± 0.005 mM in 5mM basolateral glucose and this decreased to 0.26 ± 0.003 mM when basolateral glucose was increased to 15mM. Addition of BrPy in the presence of 5mM basolateral glucose increased intracellular glucose concentration to 0.72 ± 0.003 mM ($p\leq0.0001$; n=83) (Figure 6B).

A similar pattern was seen in HBEC grown at air-liquid interface. Intracellular glucose concentration was 0.09 ± 0.002 mM in 5mM glucose and this decreased to 0.03 ± 0.001 mM when basolateral glucose concentration was raised to 15 mM (n=150) (Figure 6C).

Glucose metabolism

Glycolysis was increased in HBEC in response to elevation of extracellular glucose concentration from 5mM to 15mM consistent with our previous observations in H441 cells

(Figure 7A) **(12)**. In addition, the amount of glycogen per culture was increased two fold after exposure to 15mM glucose (from 9.1±1.3 to 20.2±1.5 mg/ml, $p<0.0001$, n=6). Inhibition of hexokinase with BrPy (100μM) reduced glycogen in H441 exposed to 15mM ($p<0.001$, n=6) but not 5mM glucose (Figure 7B). Thus, elevation of extracellular glucose increased hexokinase driven glycolysis and glycogen synthesis.

Hexokinase-independent pathways are also present in airway cells, such as the polyol pathway, which utilises aldose reductase to convert glucose to sorbitol. Such a pathway could also contribute to maintaining low intracellular glucose in the face of increased extracellular glucose. There was no significant difference in mean intracellular sorbitol between cells grown in 5 or 15 mM glucose. However, inhibition of hexokinase activity with BrPy in the presence of 15mM glucose caused a small but significant elevation of sorbitol (from 0.04±0.001 to 0.05±0.002, $p<0.01$, n=8). This elevation was inhibited by the aldose reductase inhibitor epalrestat (30μM) (n=8) (Figure 7C). These data indicate that under circumstances when intracellular glucose rises, the sorbitol pathway can contribute to glucose utilisation in these cells.

Airway surface liquid glucose

Glucose in washes from the ASL of cell cultures grown at air-liquid interface were increased from 3.6±0.7 to 45.2±1.7 μM, $p<0.001$, n=4 and 7 respectively) when basolateral glucose was raised from 5 to 15 mM for 6 hours. Taking into account the original volume of ASL, these values approximate to 0.5mM and 6mM respectively, similar to previously published values (12). Treatment with BrPy had no further effect on ASL glucose concentrations. Transepithelial electrical resistance (TEER) was unaffected by treatments.

Discussion

Both H441 and primary HBEC expressed all three isoforms of hexokinase (HKI, II and III). This finding was consistent with that described for lung tissue but now further localises these isoforms to airway epithelial cells (24). HKI is found in most cells and is thought to be the key enzyme driving oxidative phosphorylation and the production of ATP whereas HKII is thought to be more limited in its expression and associated with insulin–sensitive tissues (9). HKIII is associated with the cytosol and nuclear periphery (32). We found that growth at air-liquid interface or elevation of glucose from 5-15 mM had no effect on the observed abundance of any of the individual isoforms consistent with the finding that HKI, II and III did not change in the lungs of alloxan–induced diabetic rats compared to wild type (24). Furthermore, we did not observe any difference in total cellular abundance of HKII in H441 cells (derived from a papillary adenocarcinoma) compared to HBEC, although it is widely accepted to be upregulated in non-small cell lung cancers (23).

HKII is a key enzyme controlling anabolic (glycogen synthesis) and catabolic (glycolysis) pathways in the cell. In muscle cells, it shuttles to the mitochondria in response to elevated extracellular glucose driving glycolysis and glycogen storage (6, 17). The pyruvate mimetic BrPy enters the cell via MCT transporters (present in H441 cells and HBEC (12)) and is a potent inhibitor of glycolysis (7, 8, 34). It is reported to decrease HKII activity by alkylating and dissociating the enzyme from the mitochondrial membrane (7, 8, 34). HKI is also associated with the mitochondrial membrane and is proposed to maintain glycolysis when extracellular glucose levels are low (17). We could find no evidence to support an effect of BrPy on this hexokinase (17). As HKIII is not bound to the mitochondria, BrPy likely has no effect on this isoform. Our finding that BrPy only inhibited 25% of total hexokinase activity

(HKI, II and III) in cell extracts would indicate that it predominantly targeted HKII activity in these cells but that total cellular hexokinase activity includes that of HKI and HKIII. The concentration effect curve for BrPy also indicated a possibility that BrPy inhibited two hexokinases with differing affinities. The initial inhibition (ie that potentially attributable to HKII) had an IC_{50} of approximately 40μM. BrPy inhibited glycolysis with a similar IC_{50} of 60 μM. Others have found similar concentrations of BrPy to inhibit glycolysis in other cell types and this has been attributed to inhibition of HKII (10, 15, 29)

We used the intracellular FRET sensor FLII12Pglu-700μΔ6 because the purified sensor was largely unaffected by pH, had the lowest K_d (660 mM) and the highest dynamic range to ascertain whether intracellular glucose could reach levels higher than that detected in ASL (~400μM)(35). The standard curve we obtained from the sensor expressed in airway cells had a similar K_d. Whilst we recognise that the measurement of intracellular glucose concentration below 100μM were towards the limit of detection with this sensor, we found that intracellular glucose concentrations were in the μM range in all our cell models. In HBEC cells grown at air-liquid interface, values were below or equivalent to concentrations we found in the airway surface liquid (~0.4 mM) *in vivo* and *in vitro* (3, 13, 37). These findings support our previous proposal that to maintain ASL glucose concentrations at this level, airway epithelial cell intracellular glucose must be similar or lower to drive glucose uptake (11, 13). We did not take the pulsed approach to changing external glucose for FRET analysis and we found that whilst there were consistent overall changes in FRET output, we also observed cyclic fluctuations in intracellular glucose that were inhibited by BrPy (18). As generation of glucose-6-phosphate by hexokinases inhibits HKII activity with high affinity (17) we suggest that this phenomenon underpins these changes (28, 36).

Cytochalacin B, which is reported to inhibit glucose transport via GLUT1, 2, 3 and 4, decreased intracellular glucose (2). Inhibition of GLUT 1 and 9 by siRNA in hepatocytes had a similar effect (35). We and others previously proposed that glucose uptake in airway cells utilised GLUT1, 2, 4 and 10 (19, 20, 25, 30). As the effect of Cytochalasin B on GLUT10 is currently unknown, we suggest that glucose moves into the airway epithelial cell at least via GLUT1/2/4 and rapid metabolism by HKII maintains low intracellular glucose.

A surprising finding of the study was that intracellular glucose decreased with extracellular hyperglycaemia. This was associated with an increase in glycolysis (12) consistent with our previous observations, glycogen synthesis and potentially other glucose utilisation pathways such as the polyol pathway. Interestingly, glycogen synthase was stimulated by hyperglycaemia in myoblasts but only when glycogen stores were depleted. The calculated glycogen content in our cells was approximately 10x lower that reported for glucose-starved myoblasts. Thus, it is possible that hyperglycaemia also stimulates glycogen synthase in airway cells (14). BrPy increased intracellular glucose concentration. As HKII was reported to respond rapidly to changes in external glucose we propose that HKII is key in directing the fate of glucose in these cells (17). However, intracellular concentration of glucose remained low in comparison to the external glucose concentration. This, together with the finding that only 25% of cellular hexokinase activity was inhibited by BrPy indicates roles for hexokinase I and III in maintaining low intracellular glucose concentration in airway cells.

Effective metabolism and low intracellular glucose in airway cells provides a driving force for glucose uptake. We propose that this helps reduce transepithelial glucose concentration gradients and aids clearance of glucose from the ASL via glucose transporters in the basolateral and apical membranes (19, 20). This work focused on short term changes in

extracellular glucose concentration. We have not yet investigated the effect of chronic elevation of glucose (as observed in poorly controlled diabetes) or in lung disease conditions such as Cystic Fibrosis where glucose metabolism is reportedly compromised (25). Nevertheless, these data support our proposal that during hyperglycaemia, glucose predominantly moves across the epithelium into the ASL via the paracellular rather than transcellular route (13, 19).

Acknowledgements

This work was funded by a MRC CASE studentship award with Astra Zeneca, Gottenburg, Sweden. J.P.G. was funded by a Respiratory Diseases Research Award from the Medical Research Foundation (Grant Reference: MRF-091-0001-RG-GARNE).

References

1. **Akunuri S, Wells C, Fisher D, Clark N, and Baker E.** Exhaled breath glucose measurements in patients with asthma and alveolitis during exacerbation and after steroid treatment.Eur Respir J 30 E520, 2007.

2. **Baines DL and Baker EM.** Glucose Transport and Homeostasisin Lung Epithelia. *in Lung Epithelial Biology in the Pathogenesis of Pulmonary Disease Eds Sidhaye, V K and Koval, M Oxford: Academic Press*: pp. 33-58., 2017.

3. **Baker EH, Wood DM, Brennan AL, Clark N, Baines DL, and Philips BJ.** Hyperglycaemia and pulmonary infection. *Proc Nutr Soc* 65: 227-235, 2006.

4. **Behjousiar A, Kontoravdi C, and Polizzi KM.** In situ monitoring of intracellular glucose and glutamine in CHO cell culture. *PLoS One* 7: e34512, 2012.

5. **Brennan AL, Gyi KM, Wood DM, Johnson J, Holliman R, Baines DL, Philips BJ, Geddes DM, Hodson ME, and Baker EH.** Airway glucose concentrations and effect on growth of respiratory pathogens in cystic fibrosis. *J Cyst Fibros*, 2006.

6. **Calmettes G, John SA, Weiss JN, and Ribalet B.** Hexokinase-mitochondrial interactions regulate glucose metabolism differentially in adult and neonatal cardiac myocytes. *J Gen Physiol* 142: 425-436, 2013.

7. **Cardaci S, Desideri E, and Ciriolo MR.** Targeting aerobic glycolysis: 3-bromopyruvate as a promising anticancer drug. *J Bioenerg Biomembr* 44: 17-29, 2012.

8. **Chen Z, Zhang H, Lu W, and Huang P.** Role of mitochondria-associated hexokinase II in cancer cell death induced by 3-bromopyruvate. *Biochim Biophys Acta* 1787: 553-560, 2009.

9. **De Gubareff T and Sleator JW.** Effects of caffeine on mammalian atrial muscle, and its interaction with adenosine and calcium. *Journal of Pharmacology and Experimental Therapeutics* 148: 202-214, 1965.

10. **Ehrke E, Arend C, and Dringen R.** 3-bromopyruvate inhibits glycolysis, depletes cellular glutathione, and compromises the viability of cultured primary rat astrocytes. *J Neurosci Res* 93: 1138-1146, 2015.

11. **Garnett JP, Baker EH, and Baines DL.** Sweet talk: insights into the nature and importance of glucose transport in lung epithelium. *Eur Respir J* 40: 1269-1276, 2012.

12. **Garnett JP, Kalsi KK, Sobotta M, Bearham J, Carr G, Powell J, Brodlie M, Ward C, Tarran R, and Baines DL.** Hyperglycaemia and Pseudomonas aeruginosa acidify cystic fibrosis airway surface liquid by elevating epithelial monocarboxylate transporter 2 dependent lactate-H+ secretion. *Sci Rep* 6: 37955, 2016.

13. **Garnett JP, Nguyen TT, Moffatt JD, Pelham ER, Kalsi KK, Baker EH, and Baines DL.** Proinflammatory mediators disrupt glucose homeostasis in airway surface liquid. *J Immunol* 189: 373-380, 2012.

14. **Halse R, Bonavaud SM, Armstrong JL, McCormack JG, and Yeaman SJ.** Control of glycogen synthesis by glucose, glycogen, and insulin in cultured human muscle cells. *Diabetes* 50: 720-726, 2001.

15. **Ho N, Morrison J, Silva A, and Coomber BL.** The effect of 3-bromopyruvate on human colorectal cancer cells is dependent on glucose concentration but not hexokinase II expression. *Biosci Rep* 36: e00299, 2016.

16. **Hopfer U, Nelson K, Perrotto J, and Isselbacher KJ.** Glucose transport in isolated brush border membrane from rat small intestine. *J Biol Chem* 248: 25-32, 1973.

17. **John S, Weiss JN, and Ribalet B.** Subcellular localization of hexokinases I and II directs the metabolic fate of glucose. *PLoS One* 6: e17674, 2011.

18. **John SA, Ottolia M, Weiss JN, and Ribalet B.** Dynamic modulation of intracellular glucose imaged in single cells using a FRET-based glucose nanosensor. *Pflugers Arch* 456: 307-322, 2008.

19. **Kalsi KK, Baker EH, Fraser O, Chung YL, Mace OJ, Tarelli E, Philips BJ, and Baines DL.** Glucose homeostasis across human airway epithelial cell monolayers: role of diffusion, transport and metabolism. *Pflugers Arch* 457: 1061-1070, 2009.

20. **Kalsi KK, Baker EH, Medina RA, Rice S, Wood DM, Ratoff JC, Philips BJ, and Baines DL.** Apical and basolateral localisation of GLUT2 transporters in human lung epithelial cells. *Pflugers Arch* 456: 991-1003, 2008.

21. **Kaminski MT, Lenzen S, and Baltrusch S.** Real-time analysis of intracellular glucose and calcium in pancreatic beta cells by fluorescence microscopy. *Biochim Biophys Acta* 1823: 1697-1707, 2012.

22. **Lee WS, Kanai Y, Wells RG, and Hediger MA.** The high affinity Na+/glucose cotransporter. Re-evaluation of function and distribution of expression. *J Biol Chem* 269: 12032-12039, 1994.

23. **Li XB, Gu JD, and Zhou QH.** Review of aerobic glycolysis and its key enzymes - new targets for lung cancer therapy. *Thorac Cancer* 6: 17-24, 2015.

24. **McLean P, Brown J, Walters E, and Greenslade K.** Effect of alloxan-diabetes on multiple forms of hexokinase in adipose tissue and lung. *Biochem J* 105: 1301-1305, 1967.

25. **Molina SA, Moriarty HK, Infield DT, Imhoff BR, Vance RJ, Kim AH, Hansen JM, Hunt WR, Koval M, and McCarty NA.** Insulin signaling via the PI3K/Akt pathway regulates airway glucose uptake and barrier function in a CFTR-dependent manner. *Am J Physiol Lung Cell Mol Physiol*: ajplung 00364 02016, 2017.

26. **Munye MM, Shoemark A, Hirst RA, Delhove JM, Sharp TV, McKay TR, O'Callaghan C, Baines DL, Howe SJ, and Hart SL.** BMI-1 extends proliferative potential of human bronchial epithelial cells while retaining their mucociliary differentiation capacity. *Am J Physiol Lung Cell Mol Physiol* 312: L258-L267, 2017.

27. **Murer H and Hopfer U.** Demonstration of electrogenic Na+-dependent D-glucose transport in intestinal brush border membranes. *Proc Natl Acad Sci U S A* 71: 484-488, 1974.

28. **Newsholme EA, Rolleston FS, and Taylor K.** Factors affecting the glucose 6-phosphate inhibition of hexokinase from cerebral cortex tissue of the guinea pig. *Biochem J* 106: 193-201, 1968.

29. **Pereira da Silva AP, El-Bacha T, Kyaw N, dos Santos RS, da-Silva WS, Almeida FC, Da Poian AT, and Galina A.** Inhibition of energy-producing pathways of HepG2 cells by 3-bromopyruvate. *Biochem J* 417: 717-726, 2009.

30. **Pezzulo AA, Gutierrez J, Duschner KS, McConnell KS, Taft PJ, Ernst SE, Yahr TL, Rahmouni K, Klesney-Tait J, Stoltz DA, and Zabner J.** Glucose depletion in the airway surface liquid is essential for sterility of the airways. *PLoS One* 6: e16166, 2011.

31. **Philips BJ, Meguer JX, Redman J, and Baker EH.** Factors determining the appearance of glucose in upper and lower respiratory tract secretions. *Intensive Care Med* 29: 2204-2210, 2003.

32. **Preller A and Wilson JE.** Localization of the type III isozyme of hexokinase at the nuclear periphery. *Arch Biochem Biophys* 294: 482-492, 1992.

33. **San Martin A, Ceballo S, Ruminot I, Lerchundi R, Frommer WB, and Barros LF.** A genetically encoded FRET lactate sensor and its use to detect the Warburg effect in single cancer cells. *PLoS One* 8: e57712, 2013.

34. **Shoshan MC.** 3-Bromopyruvate: targets and outcomes. *J Bioenerg Biomembr* 44: 7-15, 2012.

35. **Takanaga H, Chaudhuri B, and Frommer WB.** GLUT1 and GLUT9 as major contributors to glucose influx in HepG2 cells identified by a high sensitivity intramolecular FRET glucose sensor. *Biochim Biophys Acta* 1778: 1091-1099, 2008.

36. **Tan VP and Miyamoto S.** HK2/hexokinase-II integrates glycolysis and autophagy to confer cellular protection. *Autophagy* 11: 963-964, 2015.

37. **Wood DM, Brennan AL, Philips BJ, and Baker EH.** Effect of hyperglycaemia on glucose concentration of human nasal secretions. *Clin Sci (Lond)* 106: 527-533, 2004.

Figure legends

Figure 1. H441 cells and HBEC express all three forms of hexokinase. Representative western blots of cell lysates from H441 cells grown on plastic (panel A) or H441 cells or HBEC grown at air-liquid interface (panel B). Lanes indicate cell type and growth conditions of either 5mM) or 15mM glucose as indicated. Proteins immunostained for Hexokinases I, II and III are indicated to the right of the blots (all approximately ~100kDa). The immunostained housekeeping protein, β-actin is also indicated (Actin) and serves as a loading control.

Figure 2. Hexokinase activity is inhibited by BrPy. A. Effect of 3-bromopyruvate concentration on hexokinase activity in cell extracts from H441 cells exposed to 5mM glucose. The dose response did not follow a classic sigmoid curve and there was an indication that the inhibition was biphasic. Two curves could be fitted to the data to reflect initial inhibition (left hand curve) with an IC_{50} of 0.04±0.01mM or overall inhibition (right hand side) with an IC_{50} of IC_{50} of 1.2±0.28 mM (n=4). B. Total hexokinase activit
y in cell extracts from control (black bar) or BrPy100μM treated cells (grey bar). Individual data points are shown with mean ± SD, **** Significantly different from control $P<0.0001$.

Figure 3. BrPy inhibits glycolysis in airway epithelial cells.
Seahorse metabolic assay of airway cells exposed to medium or different concentrations of BrPy (1μM-1mM) as indicated to right hand side of graphs. A. Oxygen consumption rate

(OCR), B extracellular acidification rate (ECAR), C. ECAR/OCR before and after injection of 5mM glucose, oligomycin or 2-DG at points indicated. D. Dose response of glycolysis to BrPy was fit with a sigmoidal curve (Df 25, r^2 0.95) with an IC_{50} of 0.06 ± 0.02 mM.

Figure 4. FRET ratio (ECFP/Citrine) was measured over a period of 6 minutes using the glucose FRET sensor FLII12Pglu-700μΔ6. A. H441 cells grown on coverslips were exposed to either osmotically balanced 5mM glucose; (filled circles) or 15mM glucose(closed triangles), both n=16. Cells were also exposed to the same conditions in the presence of the hexokinase inhibitor BrPy shown as open circles or open triangles respectively (both n=14). B. FRET ratio (ECFP/Citrine) for H441 cells grown at air-liquid-interface and exposed to either 5mM glucose (filled circles, n=12) or 15mM glucose (closed triangles, n=6). Cells were also exposed to 5mM in the presence of the hexokinase inhibitor BrPy shown as open circles (n=4). C. FRET ratio (ECFP/Citrine) in HBEC grown at air-liquid-interface, exposed to either osmotically balanced 5mM glucose (filled circles, n=12) or 15mM glucose (closed triangles, n=15) D. FRET ratio (ECFP/Citrine) glucose dose response curve for cells shown in A, equilibrated with extracellular glucose as described in Results. Data points are shown as means only in A, B and C for clarity. **** Significantly different $p<0.0001$ between groups as indicated. Data in D is shown as mean ± SD Data were fitted with a sigmoidal 1 site binding curve Df 37, r^2 0.6 Values shown in A and B are directly comparable but FRET ratio values in A, B and C cannot be directly compared because of the different imaging conditions required for the two cell types and their growth substrates.

Figure 5. Inhibition of cellular glucose uptake increased FRET ratio indicating a decrease in intracellular glucose concentration. H441 cells grown at air-liquid interface (ALI) and exposed to either 5mM glucose or 15mM glucose in the absence or presence of the

facilitative glucose transport inhibitor Cytochalasin B (CytoB). Individual data points are shown with mean ± SD. **** Significantly different p<0.0001, n=24 between groups as indicated.

Figure 6. Intracellular glucose concentration calculated from FRET ratio dose response curves. A. Calculated intracellular glucose concentration in H441 cells grown on plastic and exposed to 5mM (filled circles) or 15mM D-glucose (15mM; hyperglycaemia, closed triangles) and in the presence of BrPy shown as open circles/open triangles. Values were calculated using the dose response curve shown in Figure 1B. Individual data points are shown with mean ± SD, ****p<0.0001; n=117, between groups as indicated. B. Calculated intracellular glucose concentration for H441 cells at grown at air-liquid interface in either 5mM glucose (filled circles) or 15mM glucose (closed triangles) or 5mM glucose in the presence of BrPy (open circles). Individual data points are shown with mean ± SD, ****P<0.0001; n=83 between groups as indicated. C. Calculated intracellular glucose for HBEC cultured at air-liquid interface in either 5mM glucose (filled circles) or 15mM glucose (closed triangles). Individual data points are shown with mean ± SD, ****P<0.0001; n=150, between groups as indicated.

Figure 7. Glycolysis, glycogen and sorbitol are increased by elevation of extracellular glucose concentration. A. Glycolysis measured in airway cells as extracellular acidification rate (ECAR) after injection of 5mM glucose (closed circles) or 15 mM glucose (closed triangles). ****P<0.0001; n=34. B. Glycogen measured in airway cells after exposure to 5mM glucose (closed circles) or 15 mM glucose (closed triangles) and BrPy (open symbols). Individual data points are shown with mean ± SD, ***P<0.001, ****P<0.0001, n=6. C. Sorbitol measured in airway cells after exposure to 5mM glucose (closed circles) or 15 mM

glucose (closed triangles) and BrPy (open symbols) or epalrestat (EP) (half shaded symbols). Individual data points are shown with mean ± SD, *P<0.05, **P<0.01, n=8

Figure 8. Paracellular diffusion drives ASL glucose concentration. A. Transepithelial electrical resistance (TEER) and B. Glucose concentration in ASL washes after exposure to 5mM glucose (closed circles) or 15 mM glucose (closed triangles) and BrPy (open symbols). Individual data points are shown with mean ± SD, ***P<0.001, ****P<0.0001, n=6. Proposed mechanism for the role of HK2 in maintaining low intracellular glucose in C. Normoglycaemia and D. Hyperglycaemia. There is a diffusion gradient for paracellular movement of glucose from the blood/interstitium to the airway surface liquid (ASL). Glucose uptake via glucose transporters (GLUT) is maintained by metabolism which generates low intracellular glucose. We propose that this occurs predominantly by HKII driven conversion of glucose to glucose-6-phosphate and glycolysis. When blood glucose levels are raised to 15mM (hyperglycaemia) there is increased paracellular movement of glucose into the ASL. Increased glucose uptake, elevates HK2 activity at the mitochondria, increasing G-6-P, glycolysis and glycogen synthesis. This effectively reduces intracellular glucose concentration which maintains a glucose gradient for clearance of glucose from the ASL and prevents transcellular efflux into the ASL. Inhibition of HKII with BrPy elevates intracellular glucose but concentrations remain low in comparison to external glucose concentration indicating additional contribution of HKI/III and the HK-independent polyol pathway to glucose metabolism.

612

613

614

615

Figure 1

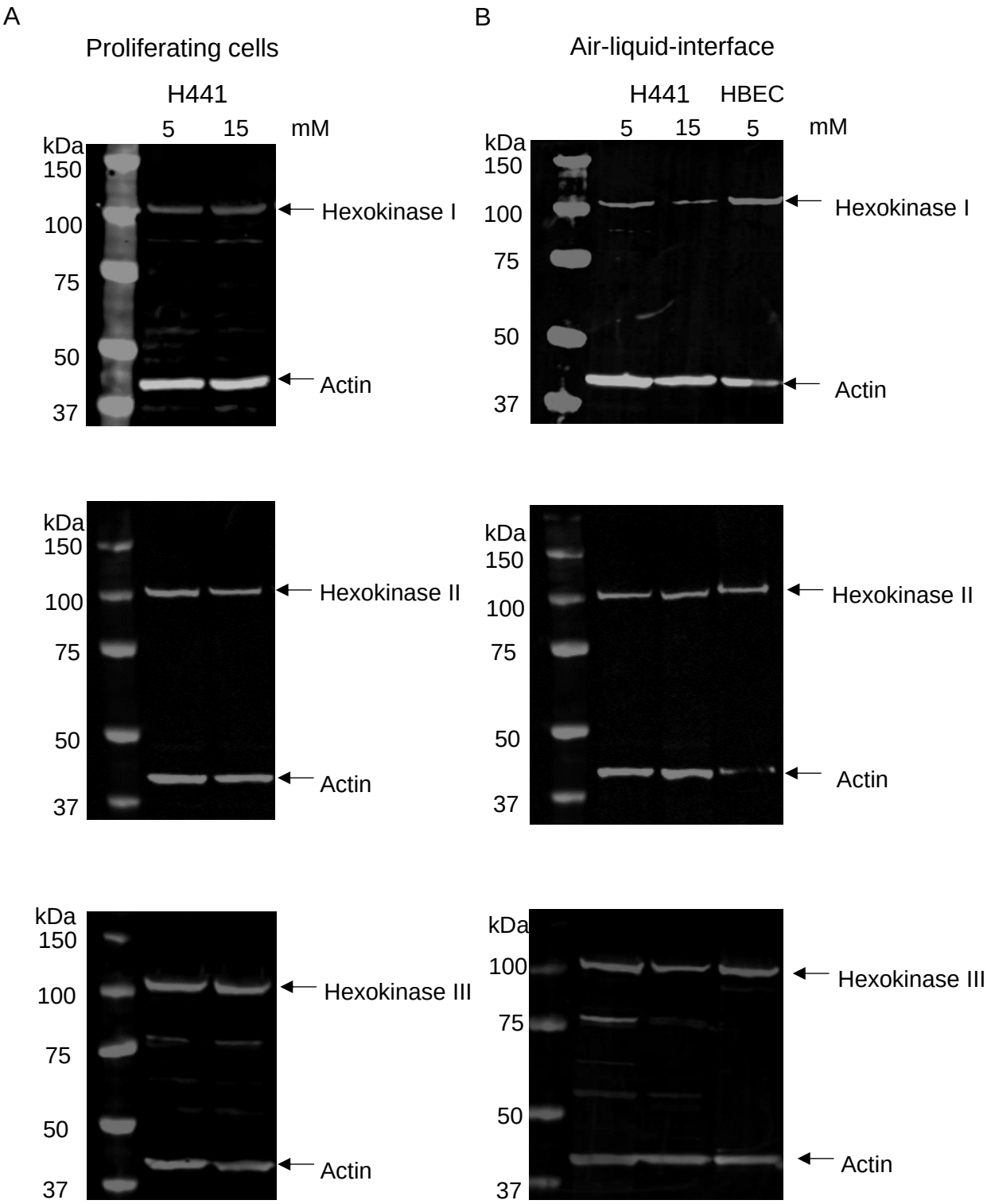
A
Proliferating cells
H441
5
15
mM
kDa
150
100
75
50
37
Hexokinase I
Actin
Hexokinase II
Actin
Hexokinase III
Actin
B
Air-liquid-interface
H441
HBEC
5
15
5
mM
kDa
150
100
75
50
37
Hexokinase I
Actin
Hexokinase II
Actin
Hexokinase III
Actin

Figure 2

A

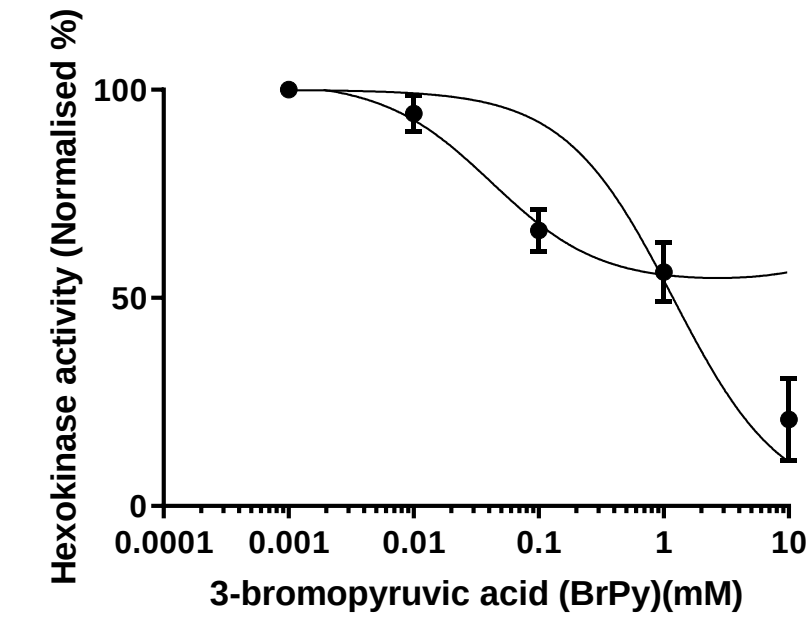
Hexokinase activity (Normalised %)
100
50
0
0.0001
0.001
0.01
0.1
1
10
3-bromopyruvic acid (BrPy)(mM)

B

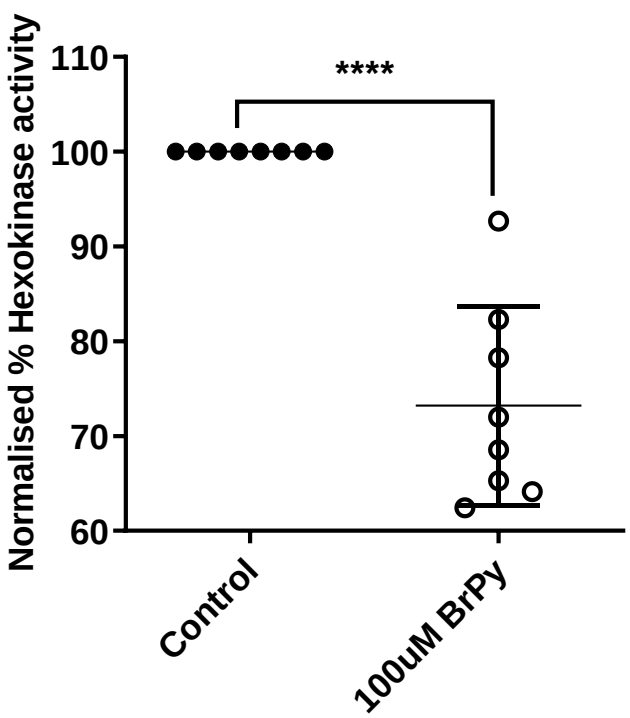
Normalised % Hexokinase activity
110
100
90
80
70
60
****
Control
100uM BrPy

Figure 3

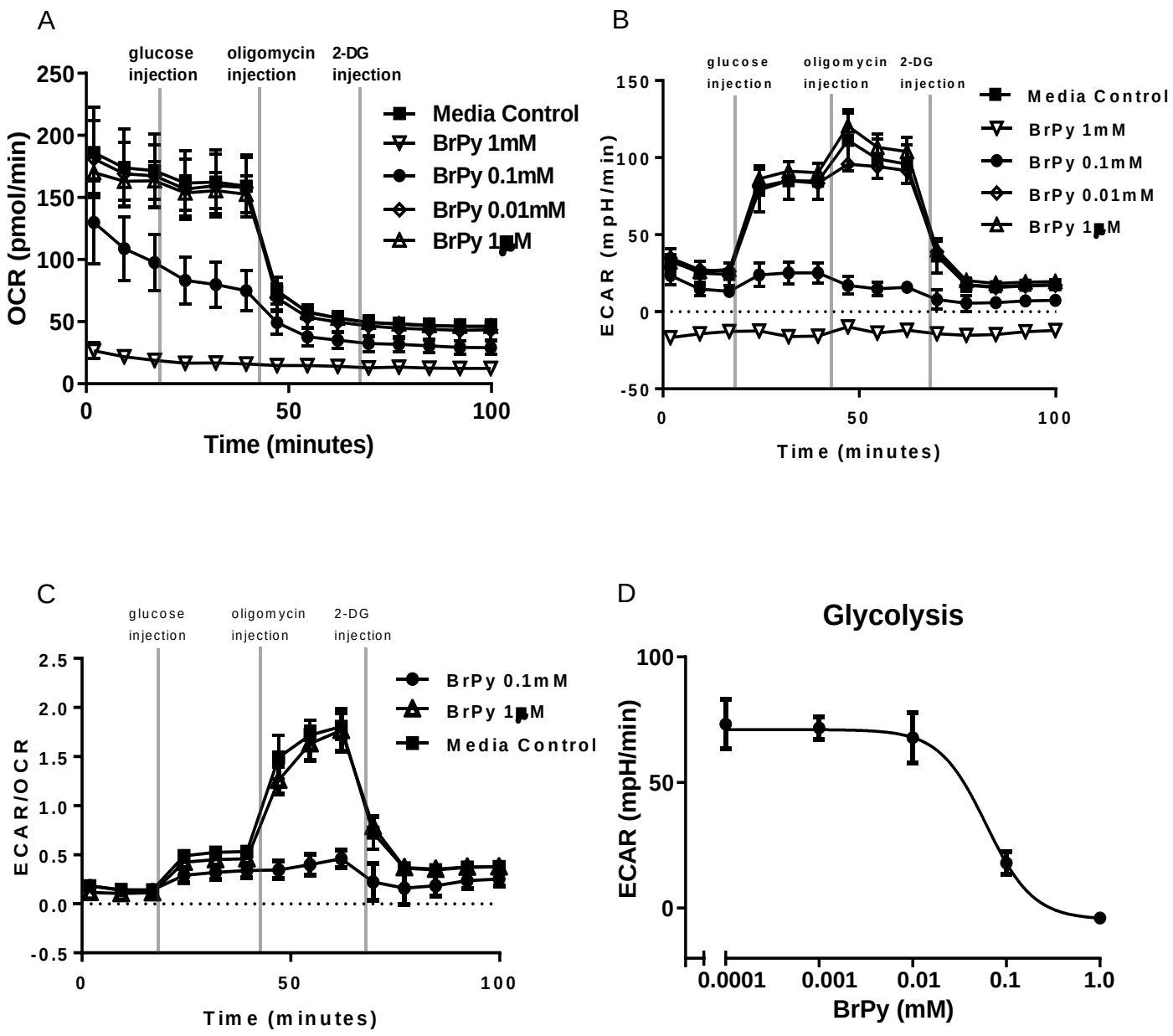
A
glucose injection
oligomycin injection
2-DG injection
OCR (pmol/min)
Time (minutes)
Media Control
BrPy 1mM
BrPy 0.1mM
BrPy 0.01mM
BrPy 1μM
B
ECAR (mpH/min)
Time (minutes)
C
ECAR/OCR
Time (minutes)
D
Glycolysis
ECAR (mpH/min)
BrPy (mM)

Figure 4

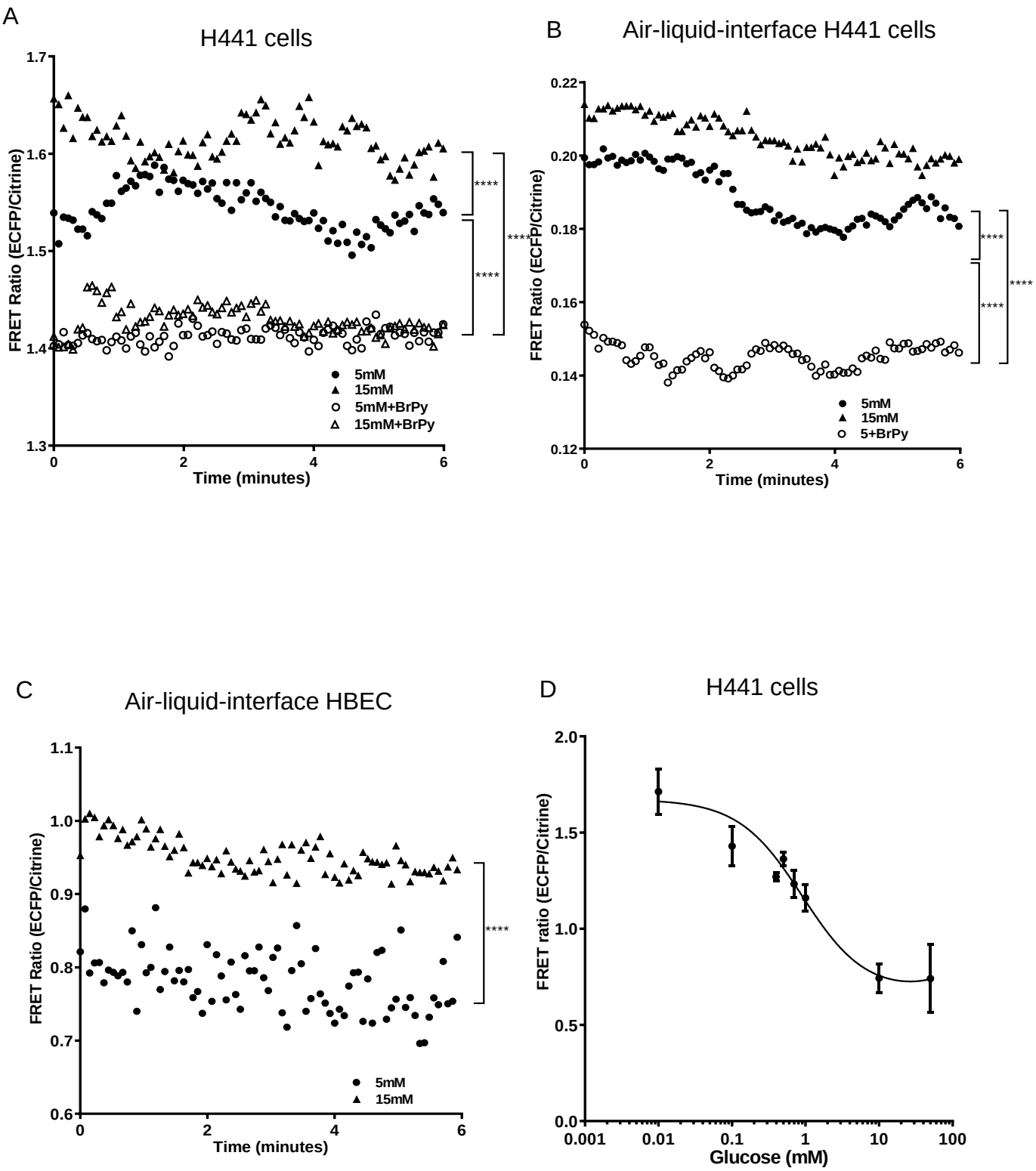
A
H441 cells
FRET Ratio (ECFP/Citrine)
Time (minutes)
5mM
15mM
5mM+BrPy
15mM+BrPy
****
B
Air-liquid-interface H441 cells
FRET Ratio (ECFP/Citrine)
Time (minutes)
5mM
15mM
5+BrPy
****
C
Air-liquid-interface HBEC
FRET Ratio (ECFP/Citrine)
Time (minutes)
5mM
15mM
****
D
H441 cells
FRET ratio (ECFP/Citrine)
Glucose (mM)

Figure 5

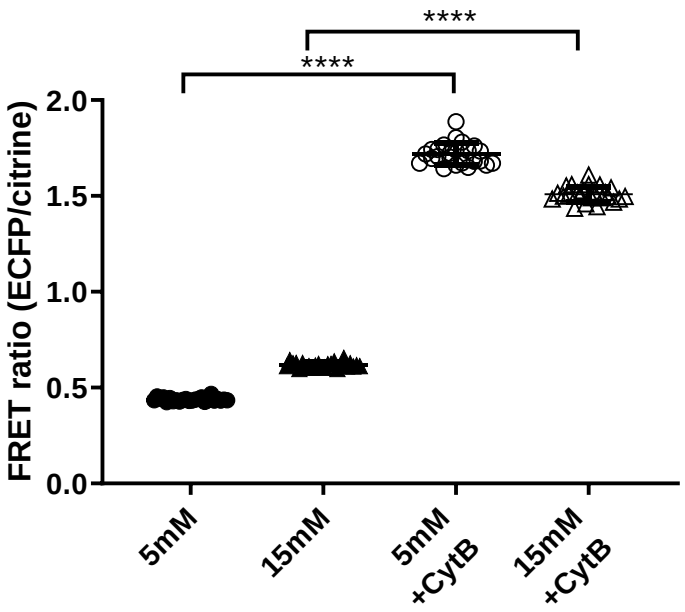
****
****
FRET ratio (ECFP/citrine)
2.0
1.5
1.0
0.5
0.0
5mM
15mM
5mM +CytB
15mM +CytB

Figure 6

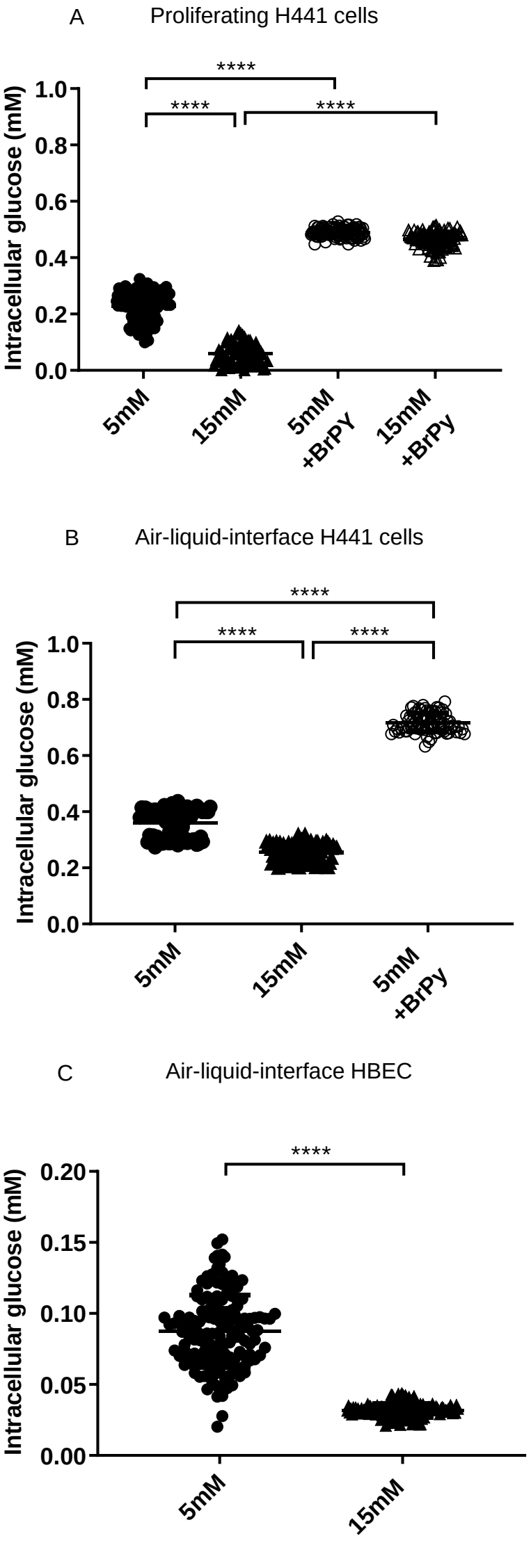
A
Proliferating H441 cells
****
****
****
Intracellular glucose (mM)
1.0
0.8
0.6
0.4
0.2
0.0
5mM
15mM
5mM +BrPY
15mM +BrPy
B
Air-liquid-interface H441 cells
****
****
****
Intracellular glucose (mM)
1.0
0.8
0.6
0.4
0.2
0.0
5mM
15mM
5mM +BrPy
C
Air-liquid-interface HBEC
****
Intracellular glucose (mM)
0.20
0.15
0.10
0.05
0.00
5mM
15mM

Figure 7

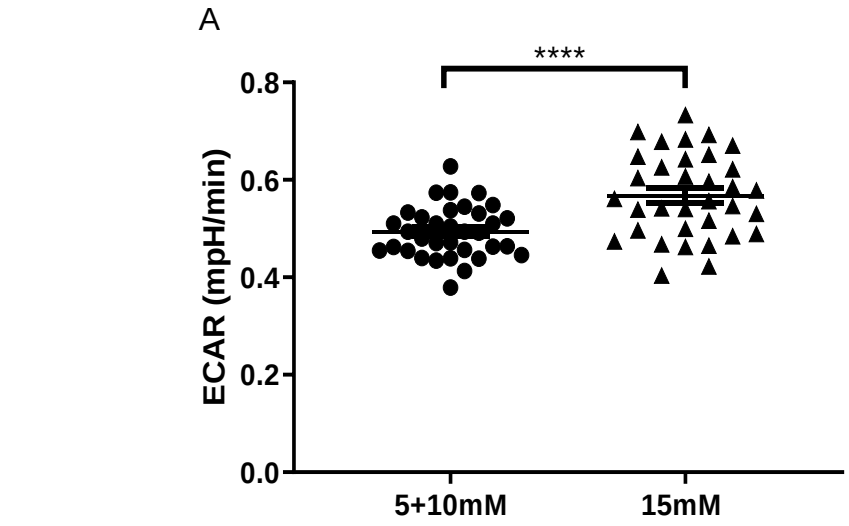
A
****
0.8
0.6
0.4
0.2
0.0
ECAR (mpH/min)
5+10mM
15mM

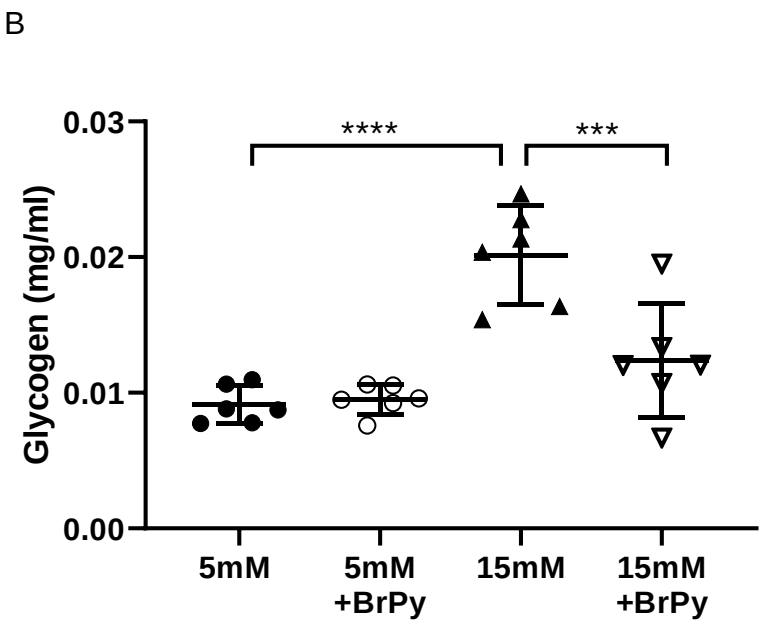
B
****
***
0.03
0.02
0.01
0.00
Glycogen (mg/ml)
5mM
5mM +BrPy
15mM
15mM +BrPy

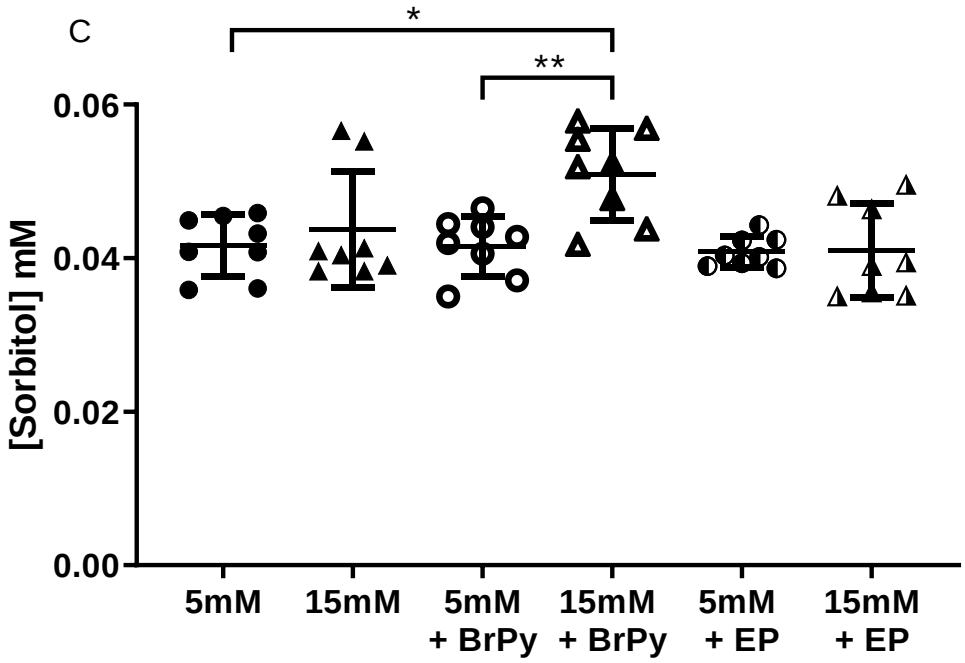
C
*
**
0.06
0.04
0.02
0.00
[Sorbitol] mM
5mM
15mM
5mM + BrPy
15mM + BrPy
5mM + EP
15mM + EP

Figure 8

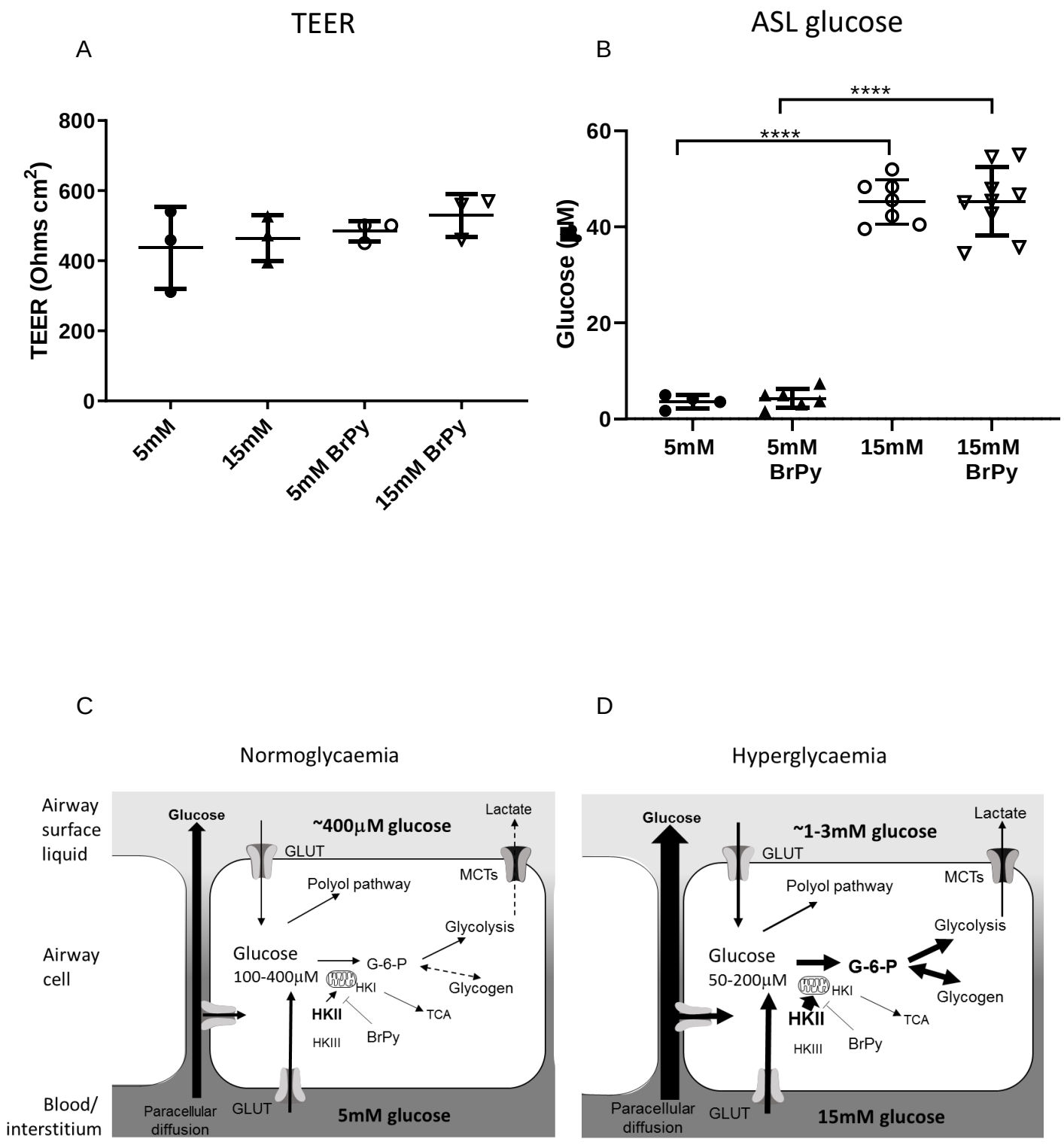
TEER
A
TEER (Ohms cm^2)
800
600
400
200
0
5mM
15mM
5mM BrPy
15mM BrPy
ASL glucose
B
Glucose (mM)
60
40
20
0
****
****
5mM
5mM BrPy
15mM
15mM BrPy

C
Normoglycaemia
Airway surface liquid
Airway cell
Blood/ interstitium
Glucose
~400µM glucose
Lactate
GLUT
MCTs
Polyol pathway
Glycolysis
Glucose
100-400µM
G-6-P
HKI
Glycogen
HKII
HKIII
BrPy
TCA
Paracellular diffusion
GLUT
5mM glucose
D
Hyperglycaemia
Glucose
~1-3mM glucose
Lactate
GLUT
MCTs
Polyol pathway
Glycolysis
Glucose
50-200µM
G-6-P
HKI
Glycogen
HKII
HKIII
BrPy
TCA
Paracellular diffusion
GLUT
15mM glucose